An Adaptive Undersampling Scheme of Wavelet-Encoded Parallel MR Imaging for More Efficient MR Data Acquisition

Hua Xie*[a], John C. Bosshard[b], Jason E. Hill[a], Steven M. Wright[b], Sunanda Mitra[a]
[a] Dept. of Electrical & Computer Engineering, Texas Tech University, Lubbock, TX 79409; [b]Dept. of Electrical and Computer Engineering, Texas A&M University, College Station, TX 77843 USA

ABSTRACT

Magnetic Resonance Imaging (MRI) offers noninvasive high resolution, high contrast cross-sectional anatomic images through the body. The data of the conventional MRI is collected in spatial frequency (Fourier) domain, also known as *k*-space. Because there is still a great need to improve temporal resolution of MRI, Compressed Sensing (CS) in MR imaging is proposed to exploit the sparsity of MR images showing great potential to reduce the scan time significantly, however, it poses its own unique problems. This paper revisits wavelet-encoded MR imaging which replaces phase encoding in conventional MRI data acquisition with wavelet encoding by applying wavelet-shaped spatially selective radiofrequency (RF) excitation, and keeps the readout direction as frequency encoding. The practicality of wavelet-encoded MRI by itself is limited due to the SNR penalties and poor time resolution compared to conventional Fourier-based MRI. To compensate for those disadvantages, this paper first introduces an undersampling scheme named significance map for sparse wavelet-encoded *k*-space to speed up data acquisition as well as allowing for various adaptive imaging strategies. The proposed adaptive wavelet-encoded undersampling scheme does not require prior knowledge of the subject to be scanned. Multiband (MB) parallel imaging is also incorporated with wavelet-encoded MRI by exciting multiple regions simultaneously for further reduction in scan time desirable for medical applications. The simulation and experimental results are presented showing the feasibility of the proposed approach in further reduction of the redundancy of the wavelet *k*-space data while maintaining relatively high quality.

Keywords: Magnetic Resonance Imaging (MRI); wavelet-encoded MR imaging; adaptive wavelet encoding; significance map; sparsity; multiband selective excitation.

1. INTRODUCTION

MRI imaging speed is critical in many applications but is limited by various factors due to physical and physiological reasons. Great effort has been devoted to improving the acquisition speed and numerous fast imaging techniques have been proposed and some of them are widely used in current scanners, e.g. fast spin-echo imaging, fast gradient-echo imaging and echo-planar imaging. Additionally, methods with reduced field of view (FOV) can further improve scan time by reducing time-consuming phase encoding steps, such as partial Fourier reconstruction utilizing the conjugate complex symmetry of *k*-space, and parallel imaging exploiting spatial sensitivity information of multiple receiving coils.

Recent research addressed the possibility of combining compressed sensing with MR imaging. Lustig et al [1] investigated the sparse representation of MR images including wavelet domain. Theoretically an appropriate incoherent sampling scheme can recover an image from its sparse representation by minimizing its $\ell 1$ norm. Such an optimal sampling scheme is difficult to achieve in practice and random undersampling in *k*-space is usually sufficient. However, it is indicated that there is still no general theoretical performance guarantee for CS MRI [2]. The CS MRI reconstruction is a convex optimization problem, which is computationally intensive, and is often performed offline. It is not possible to have real-time image reconstruction to visually inspect the image quality during scan. Hence CS MRI is still limited to research purposes because it usually results in MR images with large residual artifacts and cannot guarantee diagnostic accuracy [3].

Non-Fourier basis spatially encoded MR imaging, on the other hand, offers an alternative way to represent the MR images in a sparse fashion and is able to describe the contents of MR images more compactly than a Fourier basis, e.g. wavelet basis. Wavelet-encoded MRI was proposed decades ago by Weaver et al [4]. The first implementation of wavelet-encoded MRI was presented by Panych et al [5], which replaced phase encoding with wavelet encoding by generating wavelet-shaped spatially selective RF excitations and kept the Fourier encoding in the readout direction. Due to the limitations of wavelet-encoded MRI which suffers from significant SNR penalties and limited temporal resolution

per se compared to Fourier encoding, its practical application is limited [6]. However, on the other hand, because of the spatial localization and the multi-resolution nature of wavelet basis, some solutions were proposed to overcome some of the limitations and take advantage of those natures [7][8][9]. An adaptive imaging algorithm was developed in [7] aiming to minimize the redundancy in data acquisition for dynamic MRI by only refreshing image data where significant change was predicted to occur. An efficient encoding scheme was introduced in [9] targeting a specific spatial and frequency range to capture the signal change caused by contrast agent uptake. Inspired by those works, we decided to revisit wavelet-encoding technique and proposed a non-adaptive wavelet undersampling scheme to exploit the compressibility of wavelet-encoded k-space, which shows that it is possible to achieve acceptable reconstruction quality with only 25% of the wavelet coefficients [10]. This paper further investigates the possibility of improving performance by adaptively generating the significance map and incorporating it with the Multiband (MB) parallel imaging technique for faster data acquisition and to make wavelet-encoded MRI more applicable.

2. METHODOLOGY

2.1 Wavelet-Encoded MRI

This section provides a brief review of the theory of the conventional Fourier and the wavelet encoding in MRI. In conventional Fourier-based MR imaging, the received signal (*k*-space) can be described as

$$S^k(k_x, k_y) = \iint \rho(x, y) e^{-2\pi i(k_x x + k_y y)} dxdy \tag{1}$$

where $\rho(x, y)$ is the effective magnetization at location (x, y) and k_x, k_y are determined by the applied gradient waveforms, while slice thickness is ignored here for simplicity.

Like the discrete Fourier transformation (DFT), the discrete wavelet transformation (DWT) is a linear invertible operation. All wavelets are translated and dilated from the mother wavelet by the relation

$$\psi_{j,n}(x) = \frac{1}{\sqrt{2^j}} \psi\left(\frac{x - 2^j n}{2^j}\right); \qquad j, n \in \mathrm{Z}, \tag{2}$$

where the dilatation and translation are denoted by j and n respectively. The idea of wavelet encoding is that a space of finite-energy can be decomposed into a hierarchy of subspaces $\{V_j\}$ of different resolution. This hierarchy is in the sense that the approximation space can be reconstructed by combining V_{j+1} and the detail space W_{j+1},

$$V_j = V_{j+1} \oplus W_{j+1}, \tag{3}$$

By repeated application of this recursive decomposition, an approximation space V_0 can be represented completely by a hierarchy of detail subspaces $\{W_j\}$, which can be reconstructed using a series of weighted wavelets. In MRI term, the wavelet encoded *k*-space S^w can be reconstructed by combining detail subspaces

$$S^w = V_0 = V_1 \oplus W_1 = V_2 \oplus W_1 \oplus W_2 = V_j \oplus W_1 \oplus W_2 \oplus \ldots \oplus W_j. \tag{4}$$

The wavelet/scaling function is in effect a band-pass filter and scaling it for each level halves its bandwidth. An infinite number of levels would be required to cover the entire field of view (FOV). The scaling function filters the j^{th} level of wavelet transform and ensures the entire spectrum is covered. The approximation space V_j can be spanned using a set of such functions $\phi_n(x)$ given by

$$\phi_n(x) = \phi_n(x - n\Delta x), b = -\frac{N}{2} \cdots \frac{N}{2} - 1, \tag{5}$$

where $\Delta x = \mathrm{FOV_w}/N$, 3-dB bandwidth of the pulse. $\mathrm{FOV_w}$ is equal to field of the view along wavelet encoding direction.

Both wavelet and scaling functions can be regarded as spatial sampling functions that excite different area within FOV. It is shown that at low flip angle, RF pulse shapes and excitation profiles are Fourier transform pairs. Hence, each wavelet/scaling functions can be generated with corresponding RF excitation pulses with different 3-dB bandwidth and

center frequency. Combining all wavelet and scaling functions in a discrete form gives the wavelet synthesis matrix *WT* which can be used for image reconstruction.

For small-flip-angle RF pulses, the wavelet-encoded *k*-space is given as

$$S_{j,n}^{w}(n,k_y)=\iint \rho(x,y)w_{j,n}e^{-2\pi ik_y y}dxdy \tag{6}$$

where $w_{j,n}$ is the excitation profile corresponding to j^{th} level wavelet decomposition and translation of $n\Delta x$.

Polynomial spline wavelets, Battle-Lemarié basis functions, are applied to decompose the image into multiply levels. Design of RF excitation pulses to generate such wavelets can be found in [11]. The reason of using this wavelet basis is that its resolution is close to the theoretical limit obtained by Fourier encoding and its Fourier transform which is used as RF excitation profiles are smooth and decay to zero quickly. The reconstruction is achieved by taking 1D inverse Fourier transform along the readout direction and inverse wavelet transform along the wavelet-encoded direction,

$$f(x,y)=WT^{-1}S^{w}FT^{-1} \tag{7}$$

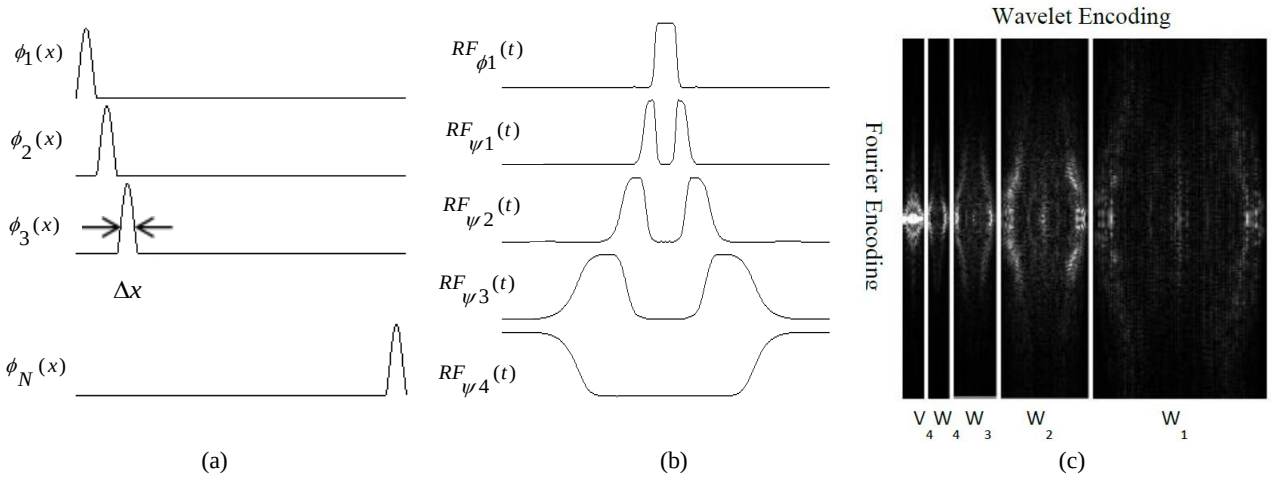

Figure 1. A set of spatially localized wavelet basis functions. (b) 4-level RF excitation pulses profile; (c) Visualization of Four-Level Wavelet Encoded k-space.

2.2 Empirical Significance Map Generation

Because of the sparsity of wavelet-encoded *k*-space, the entire FOV is not needed for image reconstruction. When the wavelet-encoded MRI was first implemented by Panych et al, the possibility of reducing the wavelet encoding steps was discussed given the spatial localization and multi-resolution properties of the wavelet transform. It is mentioned in [2] that an empirical estimate of the sparsity can be obtained with proper constraints by performing trials. Our previous work [10] shows that it is possible to achieve acceptable reconstruction quality with only 25% of the wavelet coefficients. One way to undersample wavelet-encoded *k*-space is via significance map generation, the term being borrowed from a well-known image compression article "Embedded image coding using Zerotrees of Wavelet coefficients" (EZW) [12]. This significance map dictates whether a column of wavelet-encoded *k*-space needs to be sampled, or in other words, whether the RF pulse generating that column is needed. Obviously, fewer number of RF pulses leads to shorter scanning time. The discrete wavelet transform provides a compact multi-resolution representation of an image so that undersampling can be achieved without degrading image quality. We developed a simpler and practical way of generating the significance map by calculating the energy of the wavelet-encoded *k*-space and only exciting the wavelets with the most energy to reduce scan time as well as maintain image quality, which can be described as following

$$\left\|S(n)\right\|_2=\sum\left|S_{j,n}^{w}(n,k_y)\right|^2,$$

$$\arg\max_{S_u(n)}\left\|S(n)\right\|_2,$$

$$s.t. \min RF \;\&\; \left| f_u(x,y) - f(x,y) \right| < \varepsilon, \tag{8}$$

where *RF* denotes the number of the RF pulses needed and is proportional to the scan time. $f_u(x,y)$ is the reconstructed image from the undersampled wavelet-encoded *k*-space, and $| f_u(x,y) - f(x,y) | < \varepsilon$ ensures the image consistency.

The significance map can be acquired from the scout scan prior to actual scan and hence can be easily incorporated into current protocols at no extra time cost. Such significance maps can be used to undersample the neighboring slices because of the high consistency of significance map. However, this method requires prior knowledge of the subject to be scanned and is purely empirical.

2.3 Adaptive Significance Map Generation

To overcome the limitation mentioned above, an adaptive undersampling scheme is proposed which does not require any prior knowledge, and progressively generates the significance map of detail levels based on the estimation from the coarse level wavelet decomposition.

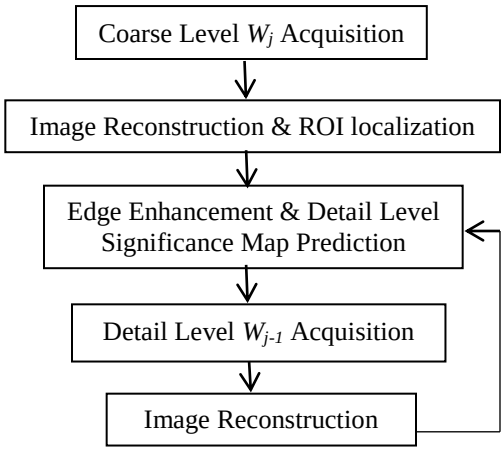

Figure 2 Adaptive wavelet-Encoded undersampling flowchart

The algorithm consists of four steps:

1. First, acquire the coarse level wavelet decomposition (V_j and W_j; j starts from four in our simulation).
2. A preliminary MR image reconstruction and any region of interest can be determined based on step 1.
3. Apply a Sobel operator for edge enhancement and apply the adaptive threshold on the estimated W_{j-1} to create an undersampling scheme for detail level wavelet coefficients.
4. Acquire the detail level coefficients and reconstruct image. Then return to step 3 until required image quality requirement is satisfied.

From an image quality point of view, edge information is of great importance but it does not necessarily contribute much energy-wise to Fourier-encoded MR images. Because of the multi-resolution feature of the wavelet transform, it is possible to estimate the edges at the finer resolution by looking at the lower resolution. To better capture the edge information, edge enhancement is applied before generating the finer level significance map so that the wavelets with more significant features such as edges will be preserved. Edge enhancement is essential because estimating Wj-1 will be trivial otherwise. With some prior knowledge of the target location information, it is feasible to automatically "zoom in" the region of interest.

This adaptive undersampling scheme requires no prior knowledge to generate the significance map and is more robust to motion. The approximate profile of the brain can be obtained from the coarse level wavelet decomposition. A soft threshold is used to determine if the region excited by a certain wavelet is out of the ROI and should be considered as background. With the same sampling rate, adaptive sampling is able to capture the edge information more faithfully than the non-adaptive method. The proposed method does not necessarily improve the SNR of the reconstruction because this method emphasizes on preserving the edges which could even lead to the reconstructed image with less energy as the region with pronounced edges may contain less energy than the region with fewer details but higher average intensity.

The brain is assumed to be noise free in the simulation but in the presence of noise, several adaptive thresholding methods can be applied [13][14].

2.4 Wavelet-encoded Multiband Parallel Imaging

It has been proposed that the scan time of wavelet MR imaging can be reduced by using a multi-slice acquisition method manipulating RF pulses [15]. Slice interference can be mitigated by acquiring interleaved slices. Further time reduction can be achieved by incorporating parallel imaging techniques e.g. SENSE [16]. Since the wavelets used have finite support and most of them do not overlap, it is also possible to obtain a much shorter repetition time (TR) and retain a long effective TR by applying a multiband (MB) RF pulse, simultaneously exciting widely spaced regions within the same slice plane so that the total number of required RF pulses is reduced. The superimposed signal is separated by the spatial sensitivity information of multiple receiving coils for correct reconstruction. Our MB concept is different from Fourier-based Simultaneous Multi-Slice (SMS) imaging [17] where a multiband composite RF pulse is simultaneously applied to excite multiple slice planes. By combining P RF pulses within one TR, the number of RF pulses needed is reduced by an acceleration factor of P, which is equal to or smaller than the number of receiving coils (N).

For the validation purpose, physically realistic sensitivity maps *SMap* are simulated using the Matlab toolbox PULSAR (http://bi.tamu.edu/software/downloads_software.htm) [19]. The array coils are modeled as rectangular loops and are assumed to be aligned along wavelet encoding direction.

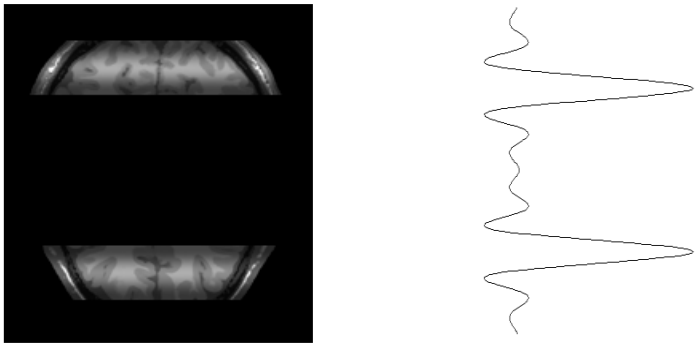

(a) (b)

Figure 3. (a) Demonstration of MB RF excitation with $P = 2$ (Non excited region is set to black to enhance contrast) (b) MB wavelet-encoded function

The received multichannel signal is a composite of P simultaneously excited regions, from which direct reconstruction using (9) yields an aliased brain with a repetition of FOV_w/P. The signal C_i acquired from coil i can be written as

$$\sum_r SMap_{i,r} \cdot x_r = C_i, \tag{9}$$

where $S_{i,r}$ is the sensitivity map of coil i from region r, and x_r is the spatially dependent complex signal of that region. The superimposed signal can be unfolded by solving (9) using least squares estimation:

$$x = SMap^{-1}C \tag{10}$$

Given the receiver coils' noise covariance ψ, the reconstruction can be rewritten as

$$x = (SMap^H \cdot \psi \cdot SMap)^{-1} SMap^H \psi^{-1} C \tag{11}$$

With the reconstruction algorithm introduced in [16], we can unfold the aliased brains and achieve an acceleration factor of P. However, the underlying inverse solution can be ill-conditioned and is affected by the acceleration factor. Tikhonov regularization has been widely used and partially solves this issue at the cost of blurring sharp edges [18].

3. RESULTS

Simulation and preliminary experimental results are presented in this section. One normal brain and one brain with multiple sclerosis (MS) lesions from McGill University Simulated Brain Database (http://brainweb.bic.mni.mcgill.ca/) are used to evaluate the performance of our proposed undersampling methods via simulation. Both brains are ideal noise-free T1-weighted with 1-mm isotropic voxel size and zero padded to make the image size of power of two. Additionally, wavelet-encoded imaging experiments on an orange were conducted at the Magnetic Resonance Systems

Lab at Texas A&M University using a 4.7T MRI system. Part of the results have been presented in our previous work [10].

3.1 Adaptive Wavelet-Encoded MRI

To evaluate the performance of the proposed adaptive undersampling scheme, Signal-to-noise ratio (SNR) of region of interest (ROI) from one normal brain and one MS brain is calculated as ROI is defined as the skull-stripped brain in this study.

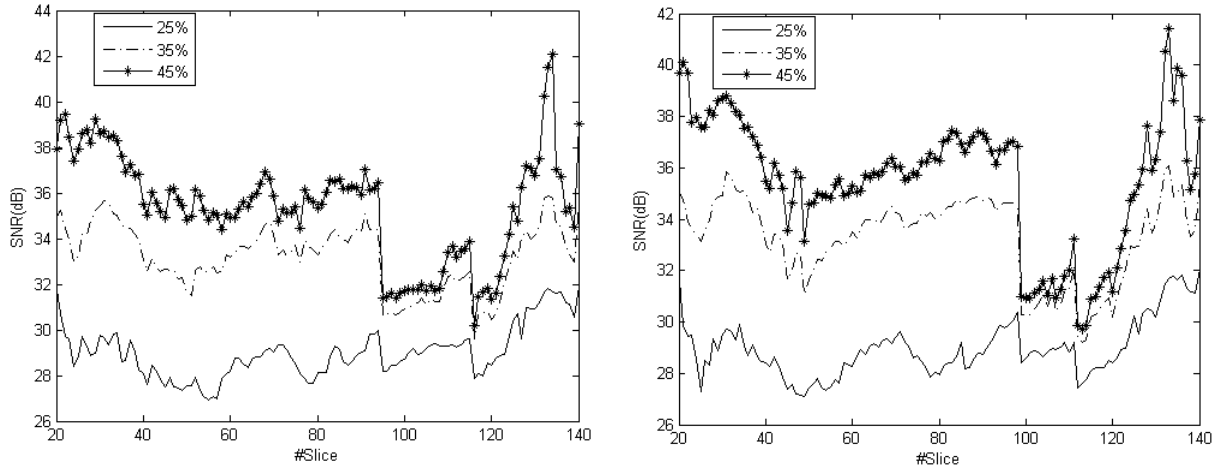

(a) (b)

Figure 4 (a) Reconstruction quality using the normal brain. Average SNR for sampling rate equal to 25%, 35% and 45% is 29.02dB, 33.20dB and 35.43dB respectively. (b) Reconstruction quality using the normal brain. Average SNR for sampling rate equal to 25%, 35% and 45% is 29.02dB, 33.20dB and 35.43dB respectively.

Inevitably there is a tradeoff between SNR and sampling rate. The simulation results shows very similar trends for normal and MS brains, and the SNR of slices between slice 95 to 120 is lower than rest of the slices which indicates higher sampling rate is needed to encode that region with more complex anatomical structure. Slice 96 of the mild MS brain is shown in Fig. 5 to verify whether undersampling affects the diagnostic quality, and slice 96 of normal brain is also shown as comparison.

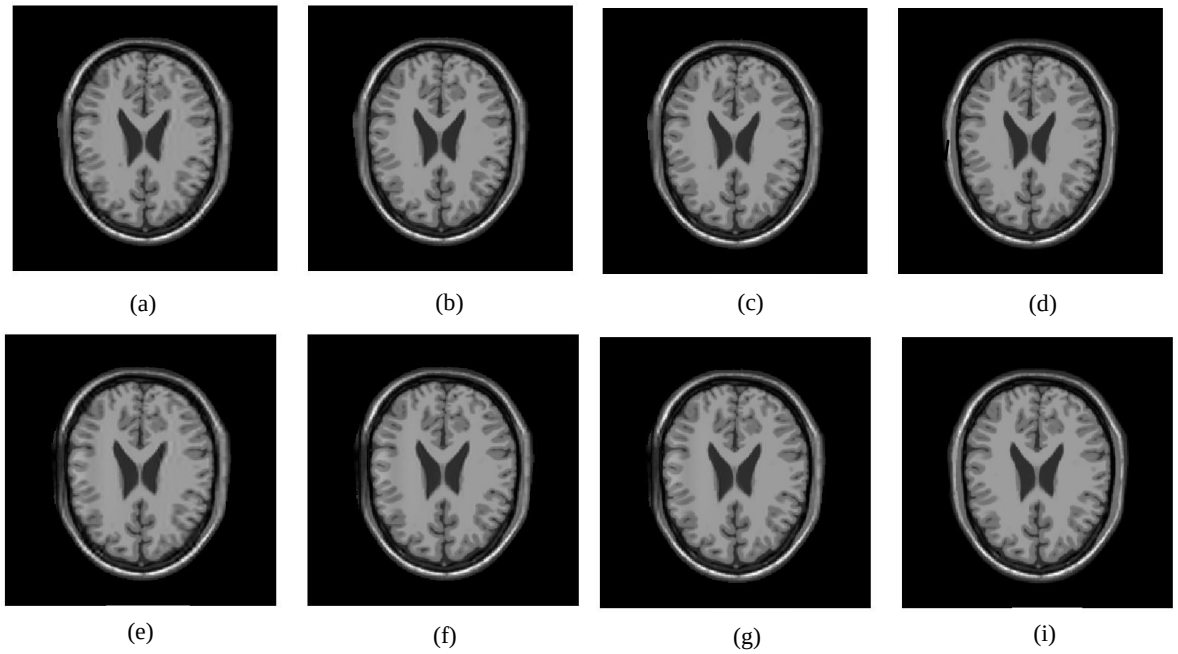

(a) (b) (c) (d)

(e) (f) (g) (i)

Figure 5. Slice 96 of MS brain with the sampling rate equal to (a) 25%, (b) 35% and (c) 45%, resulting SNR of 29.85dB, 34.63dB and 36.96dB respectively. The MS lesion is pointed with an arrow in the fully sampled reference image (d). The MS is clearly seen with all undersampling rate. As comparison, slice 96 of normal brain with the sampling rate equal to (e) 25%, (f) 35% and (g) 45%, resulting SNR of 28.18dB, 30.72dB and 31.44dB respectively. The reference image of the normal brain is shown in (i).

The simulation results show that without any prior information, the proposed adaptive undersampling scheme is able to effectively exploit the sparsity of wavelet-encoded k-space. A fourfold increase in temporal resolution can be achieved without affecting the image quality.

3.2 Wavelet-encoded Multiband Parallel Imaging

Combining multiband RF pulse parallel imaging with the adaptive undersampling scheme, the scan time can be further reduced to 1/P where P is the acceleration factor. In the simulation, 2D Gaussian profiles are assumed for the sensitivity map and the noise is not taken into consideration:

$$SMap_i(x,y) = \exp\left(\frac{-(x-x_i)^2}{2\delta_{xi}^2} - \frac{(y-y_i)^2}{2\delta_{yi}^2}\right) \tag{12}$$

where $SMap_i(x,y)$ is the simulated sensitivity map of coil i at location x, y , and x_i, y_i denote the center location of the coil, and δ_{xi} and δ_{yi} are the variance factors along x and y direction respectively.

Using the equation (10) to unfold aliased signal, the proper reconstruction can be achieved and SNR is calculated to evaluate the performance of the proposed acceleration method with different acceleration factors (P = 2, 4). Slice 96 of the normal brain is shown in the figure 6 as an example, no visual difference can be observed with either acceleration factor.

(a) (b) (c)

Figure 6. MB reconstruction. (a) P = 2, SNR = 43.22dB. (b) P = 4, SNR = 40.69dB. (c) reference image (slice 96 of the normal brain).

The SNR within ROI drops slightly as the acceleration factor P increases, because Battle-Lemarié wavelets are not well spatially localized and there is some overlap of the side lobes. This overlap does not significantly degrade reconstruction quality as long as P is no more than 4. The large acceleration factor (P>4) may pose problems on designing practical MB RF pulse and the hardware since the bandwidth and center frequency have to be highly accurate which is quite demanding on the RF coils. The SNR plot in figure 7 suggests that even at the acceleration rate of 4, the reconstruction is still relative good (minimum SNR > 36dB) as far as the simulation concerns.

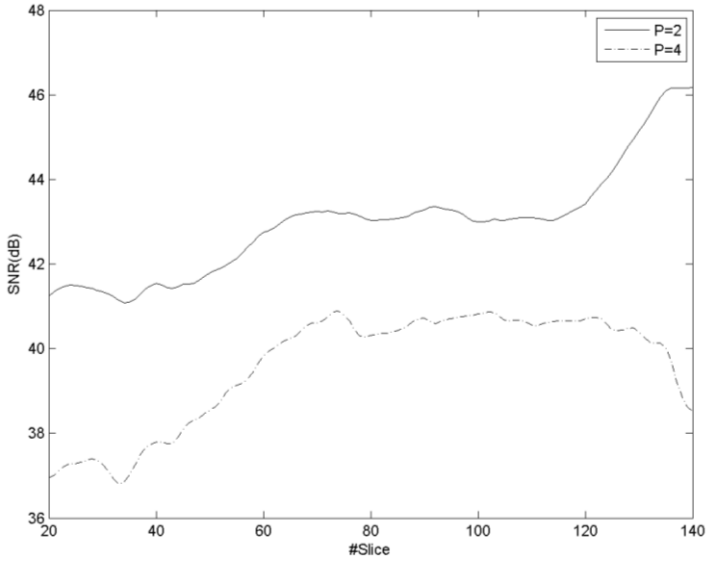

Figure 7. MB reconstruction quality of normal brain from slice 20 to 140 with $P = 2$ and $P = 4$.

However, as mentioned above, the reconstruction quality relies heavily on two factors. One is the accuracy of the MB RF pulse generated, and the other is the accuracy of the sensitivity map estimation. Moreover, the MB reconstruction may also be ill-posed in some cases. Those issues need further investigation.

3.3 Experimental results

Wavelet encoded imaging experiments were conducted at the Magnetic Resonance Systems Lab at Texas A&M University with a 4.7T MRI system [10]. The four-level Battle-Lemarié wavelets with 256 wavelet encoding steps and frequency encoding steps were implemented with TR = 3000ms, TE = 32ms, FOV = 128 mm x 128 mm, Number of Signal Averages (NSA) = 8 and tip angle = 10°. A Fourier reference image (flip angle = 90°, NSA=1) was acquired at the same resolution (Fig. 2a). This experiment serves to validate the undersampled wavelet encoded MRI technique. The preliminary result shows that the quality of the undersampled reconstruction is acceptable keeping 25% of the encoding steps. The imaging time could be greatly reduced combining the MB acceleration technique and better quality could be achieved with more optimized pulse sequence design.

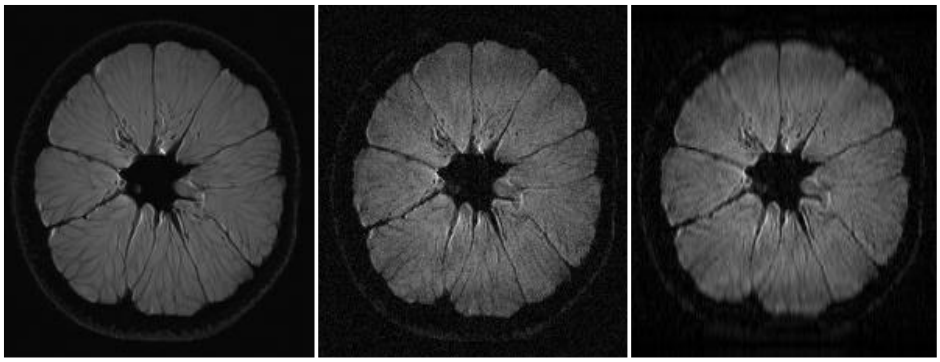

(a) (b) (c)

Figure 8 (a) Conventional Fourier reconstruction with spin echo (SNR = 36.55dB). (b) Full Wavelet reconstruction (SNR = 20.34dB). (c) Undersampled wavelet reconstruction (Sampling rate 25% SNR = 14.55dB)

4. CONCLUSIONS

To overcome some of the limitations of wavelet-encoded MRI, an adaptive wavelet undersampling scheme and wavelet-encoded MB parallel imaging algorithm are proposed to reduce the redundancy of wavelet-encoded *k*-space. The adaptive wavelet undersampling scheme proposed does not require any prior knowledge and can adaptively adjust the significance map. Fourfold increase in imaging speed is achieved with minor loss of the image quality via our MB approach. Simulation and preliminary experimental results show that the proposed methods can reduce the wavelet encoding steps significantly while maintaining image quality. Future work will focus on implementing and optimizing the proposed methods.

REFERENCES

[1] Lustig, Michael, David Donoho, and John M. Pauly. "Sparse MRI: The application of compressed sensing for rapid MR imaging." Magn Reson Med 58.6 (2007): 1182-1195.

[2] Haldar, Justin P., Diego Hernando, and Zhi-Pei Liang. "Compressed-sensing MRI with random encoding." IEEE Trans. Med. Imag 30.4 (2011): 893-903.

[3] Sung, Kyunghyun, and Brian A. Hargreaves. "High-frequency subband compressed sensing MRI using quadruplet sampling." Magn Reson Med 70.5 (2013): 1306-1318.

[4] Weaver, John B., et al. "Wavelet-encoded MR imaging." Magn Reson Med 24.2 (1992): 275-287.

[5] Panych LP, Jakab PD, Jolesz FA. “Implementation of wavelet-encoded MR imaging”. J Magn Reson Imaging 1993; 3:649–655.

[6] Panych, Lawrence P. "Theoretical comparison of Fourier and wavelet encoding in magnetic resonance imaging." *IEEE Trans. Med. Imag* 15.2 (1996): 141-153.

[7] Panych, Lawrence P., and Ferenc A. Jolesz. "A dynamically adaptive imaging algorithm for wavelet-encoded MRI." Magn Reson Med 32.6 (1994): 738-748.

[8] Wendt, Michael, et al. "Dynamic tracking in interventional MRI using wavelet-encoded gradient-echo sequences." IEEE Trans. Med. Imag 17.5 (1998): 803-809.

[9] Shimizu, Kenji, et al. "Partial wavelet encoding: a new approach for accelerating temporal resolution in contrast-enhanced MR imaging." J Magn Reson Imaging 9 (1999): 717-724.

[10] Hua Xie, John C. Bosshard, Jason E. Hill, Steven M. Wright, Sunanda Mitra, “A Novel Undersampling Scheme of Wavelet-Encoded MR Imaging”, presented at the 37th Annual Int. Conf. of IEEE EMBS, Milan, Italy, Aug. 25-29, 2015.

[11] Liu, Zheng, Brian Nutter, and Sunanda Mitra. "Fast magnetic resonance imaging simulation with sparsely encoded wavelet domain data in a compressive sensing framework." Journal of Electronic Imaging 22.2 (2013): 021009-021009.

[12] Shapiro, Jerome M. "Embedded image coding using zerotrees of wavelet coefficients." IEEE Trans. Signal Process 41.12 (1993): 3445-3462.

[13] David L. Donoho and Iain M. Johnstone. Adapting to unknown smoothness via wavelet shrinkage. J. Am. Statist. Assoc., pages 1200–1224, 1995.

[14] T.T. Cai and B.W. Silverman. Incorporating information on neighbouring coefficients into wavelet estimation. Sankhya Ser A, 63, 2001.

[15] Gelman, Neil, and Michael L. Wood. "Wavelet encoding for 3D gradient ‐ echo MR imaging." Magn Reson Med 36.4 (1996): 613-619.

[16] Pruessmann, Klaas P., et al. "SENSE: sensitivity encoding for fast MRI." Magn Reson Med 42.5 (1999): 952-962.

[17] Feinberg, David A., and Kawin Setsompop. "Ultra-fast MRI of the human brain with simultaneous multi-slice imaging." J Magn Reson Imaging 229 (2013): 90-100.

[18] Tikhonov, Andreĭ Nikolaevich, and Vasiliĭ ĬAkovlevich Arsenin. Solutions of ill-posed problems. Vh Winston, 1977.

[19] Ji, Jim X., Jong Bum Son, and Swati D. Rane. "PULSAR: A Matlab toolbox for parallel magnetic resonance imaging using array coils and multiple channel receivers." Concept Magn Reson B 31.1 (2007): 24-36.